



ELSEVIER

Nuclear Instruments and Methods in Physics Research A 443 (2000) 277–286

---

**NUCLEAR  
INSTRUMENTS  
& METHODS  
IN PHYSICS  
RESEARCH**  
Section A

---

www.elsevier.nl/locate/nima

# Analysis of alpha-emitting isotopes in an inorganic scintillator

J.C. Barton<sup>1</sup>, J.A. Edgington\**Department of Physics, Queen Mary and Westfield College, London E1 4NS, UK*

Received 30 March 1999; 31 March 1999

---

## Abstract

Large scintillating crystals are used in searches for dark matter and other elusive phenomena where the presence of trace radioisotopes is a major source of background. We describe a method for determining alpha-emitters present in concentrations very much less than  $10^{-12}$ . The optimal filter for pulse shape discrimination, described by Gatti nearly 40 years ago, is implemented using modern digital techniques. Results are presented for a large NaI(Tl) scintillator; we give a detailed quantitative analysis of its radio-impurities, showing that the  $^{235}\text{U}$  series is essentially absent and that both the  $^{232}\text{Th}$  and  $^{238}\text{U}$  series are far from equilibrium, the main contaminants being the radium isotopes and their short-lived daughters. © 2000 Elsevier Science B.V. All rights reserved.

*PACS:* 29.40.Mc; 23.60.+e; 95.35.+d*Keywords:* Scintillator; Radiopurity; Pulse-shape discrimination (PSD); Actinides; Secular equilibrium

---

## 1. Introduction

The residual counting rate in a well-screened scintillator is largely due to radioactive impurities in the scintillating material. This is notably the case for the inorganic halides. The high scintillating efficiency of these materials leads to their widespread use in studies of rare processes with low-energy deposition, such as double beta-decay [1], and in searches for dark matter in the form of weakly interacting massive particles, WIMPs (see, for example, Refs. [2–4]). The sensitivity of such experiments is partly limited by the presence of natu-

ral radioactivity. Work is in progress to improve the purity of sodium iodide [5]; here we describe the techniques used to identify and measure the residual radioactive content. Although  $^{40}\text{K}$  is an ubiquitous impurity, present at levels of  $10^{-9}$ – $10^{-10}$  by weight in the best crystals, this paper is particularly concerned with alpha-emitters. Not only are the many X-rays in the actinide decay chains a serious low-energy background; equally importantly, the characteristic signature of a WIMP interaction is the scintillation pulse profile of the recoil nucleus. Comparison [4] of neutron-induced recoils and gamma rays shows that recoil nuclei, though of much lower energy, have profiles quite similar to alpha pulses.

Most studies of alpha-emitters in scintillators have assumed that the U and Th decay chains are in equilibrium. As shown by Barton [6] in a preliminary account of our technique, this is an unsound assumption. For quantitative studies of

---

<sup>1</sup> Also at Birkbeck College, University of London, UK.

\*Corresponding author. Tel.: 44-171-975-5031; fax: 44-171-981-9465.

E-mail address: j.a.edgington@qmw.ac.uk (J.A. Edgington)

the efficiency of purification, and of residual background levels, it is important to distinguish and measure as many different isotopes as possible. Fortunately the U and Th decay chains include characteristic sequences of short-lived alpha-emitting isotopes. Thus we select alpha decays according to their distinctive pulse profiles while simultaneously recording the time of each event. From the resulting sets of time-correlated pulses one can unambiguously select and identify those due to one or other of these sequences and so determine the individual isotopic abundances.

We use a digital oscilloscope to record each individual pulse, which we subsequently analyse using the digital equivalent of the method of Gatti [7] and Martini and Gatti [8]. In this method one forms the function  $g(t) = [\gamma(t) - \alpha(t)]/[\gamma(t) + \alpha(t)]$ , where  $\gamma(t)$ ,  $\alpha(t)$  are pulse profiles due to ionisation induced by gamma-rays (or electrons) and alpha particles, respectively. For each pulse profile  $f(t)$  the discriminating parameter  $S = \Sigma g(t)f(t)$  is calculated. Gatti showed that this choice of  $S$  gives maximum discrimination  $D_{\gamma\alpha}$  between gamma and alpha pulses, where

$$D_{\gamma\alpha} = [S_\gamma - S_\alpha][\sigma^2(S_\gamma) + \sigma^2(S_\alpha)]^{-1/2}.$$

In practice it is difficult to design an analogue circuit to realise the continuous function  $g(t)$  but very simple to carry out the equivalent discrete operation once the pulses have been digitised. A preliminary account has been given by Barton [6]. The technique has been applied to scintillating crystals prepared for the UK Dark Matter Collaboration [4] and subsequently extended to include study of time-correlated pulses and hence obtain quantitative information about non-equilibrium in the actinide decay chains. Most of this work has been carried out using a large (3.6 kg) single crystal of NaI(Tl) grown and encapsulated by Quartz et Silice. The rest of this paper explains the method in detail, discusses the results obtained with this particular crystal, and considers prospects for further progress.

## 2. Experimental method

The experiments described here were carried out in a basement laboratory at Queen Mary and

Westfield College. The total cosmic ray rate was about 25% lower than on the roof but, because of the complicated geometry, it is not possible to make a reliable estimate of the equivalent absorber thickness. The scintillator crystal, 127 mm in diameter and 76 mm thick, was operated with its axis horizontal in a lead cavity which provided a minimum screening thickness of 100 mm in all directions. A silica light guide of 126 mm diameter and the same length was in optical contact with the window of the scintillator and of the similar diameter photomultiplier (Electron Tubes 9030). The output from the collector was fed via a high voltage coupling capacitor and a 50  $\Omega$  cable directly to a LeCroy 9410 digital storage oscilloscope so that the shape of the scintillation pulses could be studied without first integrating them.

Digital oscilloscopes provide both high and stable performance in a pulse shape discrimination system. For studying sodium iodide pulses we have found that sampling at 10 ns intervals for a total time of 1.8  $\mu$ s provides adequate data. The 9410 oscilloscope, like most others with sampling rates of 100 Ms/s or higher, uses only 8-bit digitisation which limits the pulse height range over which good discrimination can be achieved; the initial experiment [6] used a 10-bit oscilloscope which is no longer marketed. Naturally occurring alpha particles range in energy from 4.0 to 8.8 MeV so at first sight this problem of dynamic range appears to be a minor one. In practice there are several factors which make it of considerable significance:

- The response of inorganic crystals to heavily ionising particles is non-linear so the range of pulse heights is greater than the range of energies;
- Pulses from gamma rays are less sharply peaked than those from alphas so their maxima must be recorded down to lower levels;
- There is always some variation in scintillation response over the volume of the crystal, and as shown below this effect is not negligible;
- The range studied must be extended both downwards, so that any contributions from alphas in the encapsulating materials can be seen, and upwards so that any interference from cosmic ray spallation effects can be recognised.

Combining these factors means that a dynamic range of at least 12:1 is required. Moreover there is a generic effect (cf. Ref. [9]) in that sampling at high rates reduces the effective number of bits, for example from 8 to just over 7 when sampling at 100 Ms/s with the LeCroy 9410. The problem then is that even the maxima of the smallest pulses will be digitised with only 3 or 4 bits precision, the remainder of the pulse having a still lower precision. The effect on the discrimination  $D_{\gamma\alpha}$  of the number of bits used to digitise the peak amplitude of each pulse has been studied in Monte Carlo simulations. Fig. 1 shows results for the pulse shapes determined in this experiment; the numbers of photoelectrons simulated are typical of those produced by the alpha particles detected in this scintillator. The absolute values obtained are not wholly reliable as the modelling was slightly simplified but the dependence of  $D_{\gamma\alpha}$  on the number of bits should be insensitive to the assumptions. Clearly the use of less than 7 bits leads to a rapid decrease in performance. Also the discrimination varies as the square root of the number of photoelectrons. These two effects combine to cause a rapid deterioration with decreasing particle energy. It is possible to operate at high gain so as to

saturate the peak region of large pulses and to study only their tail regions, but we have found that, without a reliable value for the total area of the pulse, an alpha of one energy is not sufficiently distinguished from a gamma of another. Instead the problem has been reduced by using a second channel on the same oscilloscope. The incoming signal is divided in a 50  $\Omega$  splitter which preserves the match but reduces the signal to the second channel by a factor of three. The two channels are set at the same gain and both waveforms are recorded. Normally data from the more sensitive channel are stored but if this channel is saturated at any point in the waveform the second channel is substituted; if both channels are saturated, neither is stored. The method was checked by special data runs in which both channel records were stored; the ratio was found to be  $2.98 \pm 0.04$ .

As mentioned in the introduction a major consideration is to preserve and record the time relationship between successive pulses. The oscilloscope's internal clock is used to record time as well as pulse height information for every pulse and these are transferred to a conventional personal computer. A limitation is the relatively sluggish performance of the standard GPIB parallel

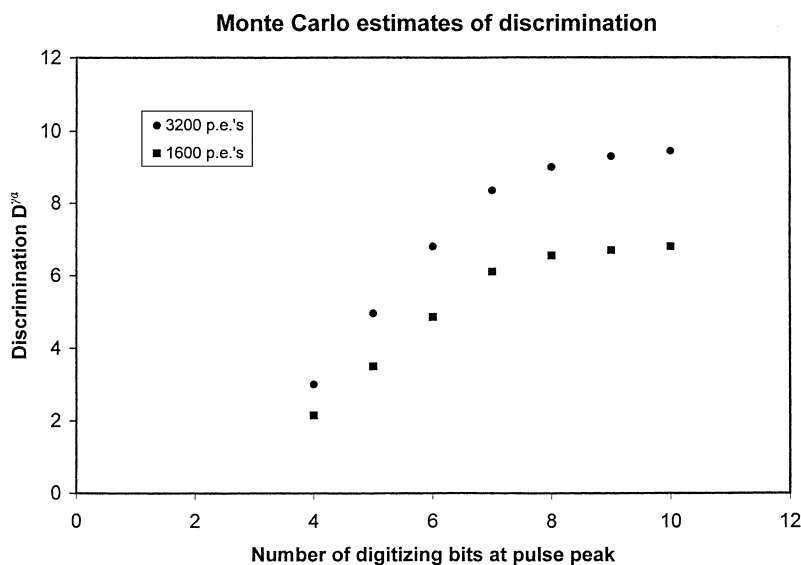


Fig. 1. Monte Carlo estimates of the expected discrimination using measured pulse shapes from gamma rays and alpha particles, sampled at 10 ns intervals. Each point was determined by 10 000 pairs of particles.

interface. Although the actual data exchange may occur at more than  $100 \text{ kbs}^{-1}$  the time taken to set up the data exchange prevents the recording of closely separated pairs of pulses. To circumvent this problem the “sequence” facility was used to record 50 individual pulses before the data for all of them was transferred to the computer. Obviously 2% of close pairs of pulses are still lost but otherwise only the normal delay before retriggering affects the data. The control program is written in C and acquires 256 data bytes for each pulse. Analysis is also done by a C program. The data reported in this paper were acquired over 30 days. The dead-time between triggers was  $75 \mu\text{s}$  and that between transfers of 50 pulses to the computer was 230 ms. The total trigger rate was  $2.72 \text{ s}^{-1}$  of which roughly one in 2000 were subsequently identified as alpha particles.

Application of the Gatti method for distinguishing gammas from alphas requires knowledge of the pulse shapes  $\gamma(t)$  and  $\alpha(t)$  for the two types of particle. These shapes depend on both the concentration of the thallium activator and the processing conditions during the growth of the crystal, so must be determined experimentally. The method used in a preliminary analysis step was first to normalise all the pulses to a constant area and then to average them. Since more than 99% of the pulses are due to gamma-rays this average provides a first estimate of their pulse shape. A second run then compares each individual pulse with this average and uses a simple chi-squared criterion to separate those pulses which are of significantly different shape. Averaging these provides a first estimate of  $\alpha(t)$ . The Gatti analysis can now be run and a discrimination value,  $S$ , allocated to each pulse;  $S$  will be positive for gamma-rays and negative for alpha particles. At this stage of the analysis a few of the pulses are doubles which show as excessively broad pulses, and pulses from Cherenkov light (produced in the light guide and windows) which are very narrow. These unwanted pulses are excluded by setting limits to the acceptable values of  $S$  so that the remaining pulses can contribute to improved estimates of the average pulse shapes. This process is iterated to provide the final estimates and classifications. We estimate that fewer than 1% of pulses classified as alphas were misidentified.

Over the range of energies used in this work the gamma pulses had a constant shape but those from alphas became slightly sharper at lower energies (Fig. 2). The small kink near 100 ns is probably a real effect and may represent an additional physical process contributing at the higher ionisation densities. However the current understanding of scintillation processes in inorganic crystals is inadequate to provide any useful interpretation of these pulse shapes.

The data from this experiment provide amplitude spectra for alpha particles and gamma-rays (Fig. 3). The gamma spectrum was calibrated by introducing a weak thorium source and so identifying the feature at channel 33 as the 2.62 MeV transition in  $^{208}\text{Pb}$ . The calibration of the alpha spectrum is less direct and is outlined in the next section.

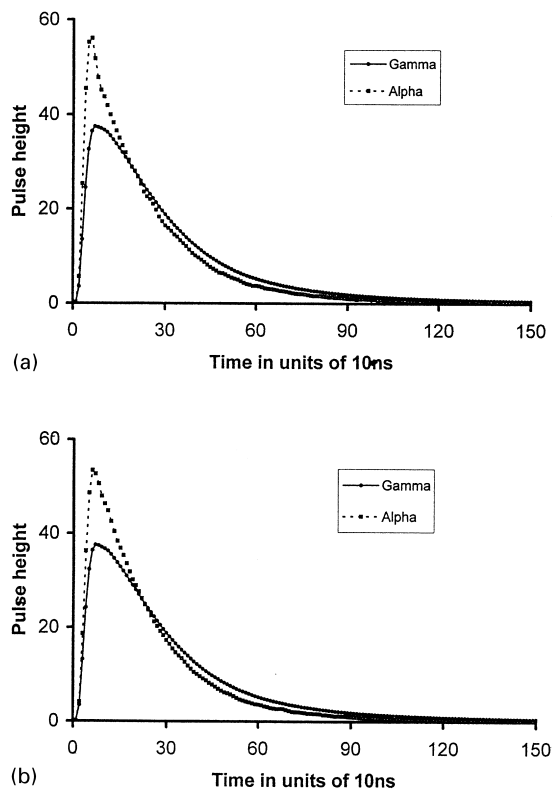


Fig. 2. The pulse shapes for gamma rays and alpha particles. The approximate gamma energies are 3 MeV in (a) and 6 MeV in (b).

### 3. Data analysis

Alpha particles in the scintillator must come from one of the three naturally occurring radioactive series. Fig. 4 shows slightly simplified diagrams of these series using data from [10]. In both the  $^{232}\text{Th}$  and  $^{235}\text{U}$  series there is a pair of alpha decays closely separated in time, and in the  $^{238}\text{U}$  series there is a  $\beta$ - $\alpha$  pair also closely separated (the short-live alpha emitters being  $^{216}\text{Po}$ ,  $^{215}\text{Po}$  and  $^{214}\text{Po}$ , respectively). The analysis program selects all  $\alpha$ - $\alpha$  events separated by  $< 1$  s, and all  $\beta$ - $\alpha$  events separated by  $< 1$  ms. The pulse height and time of all alpha pulses is recorded in a 10-deep FIFO store so that the sequence of alpha pulses prior to any close  $\alpha$ - $\alpha$  or  $\beta$ - $\alpha$  pair can be studied. The double-headed arrows in Fig. 4 indicate the triplets which should be seen for the  $\alpha$ - $\alpha$  events, and the more complicated events preceding the  $\beta$ - $\alpha$  pairs. It is not possible to study previous  $\beta$ -decays as there is a large number of unrelated pulses. There are far fewer uncorrelated  $\alpha$ -decays although their number does become significant over the longer look-back time used for the  $\beta$ - $\alpha$  pairs.

#### 3.1. $\alpha$ - $\alpha$ pairs: the $^{232}\text{Th}$ and $^{235}\text{U}$ series

There were 135  $\alpha$ - $\alpha$  pairs. Of these 14 had no other alpha pulse within the previous 300 s while 108 showed a sequence of three pulses which were compatible with the  $^{224}\text{Ra}$ - $^{220}\text{Rn}$ - $^{216}\text{Po}$  decay sequence in the  $^{232}\text{Th}$  series. The remainder had more than three alpha pulses within the analysis interval so identification of the first of the three correlated pulses was ambiguous. From the measured rate of alpha pulses one would expect about 10 of the  $\alpha$ - $\alpha$  pairs to be accidentals. Examination of each recorded event in the ambiguous sequences showed that 8 of the  $\alpha$ - $\alpha$  pairs had pulse heights whose ratio was clearly incorrect and which were regarded as accidental coincidences and removed from the analysis.

The possibility that some events were from the  $^{235}\text{U}$  series was next examined. The half-life of  $^{215}\text{Po}$  (1.78 ms) being so much shorter than that of  $^{216}\text{Po}$  (145 ms), attention was paid to the 5 events in which the separation of the  $\alpha$ - $\alpha$  pair was less than 10 ms. All of these were triple- $\alpha$  sequences. In

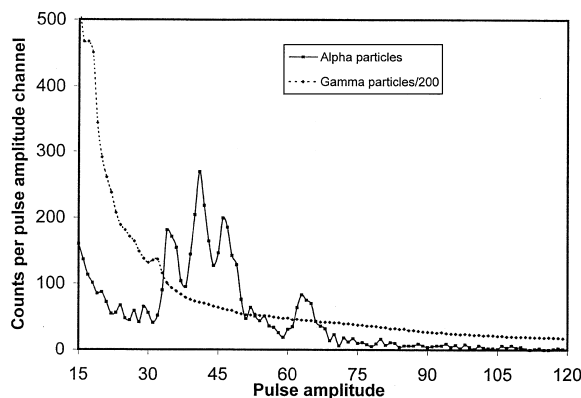


Fig. 3. Amplitude spectra, in arbitrary units, for gamma and alpha pulses; the number of gamma pulses has been divided by 200. The measured quantity is the total area under the pulse profile from 0 to 1.80  $\mu\text{s}$ . Its statistical precision is typically  $\pm 2\%$  for the alpha pulses measured here. The raw data have been re-binned into channels of similar width.

each case the amplitudes of the  $\alpha$ - $\alpha$  pairs were consistent with those of the majority ( $^{232}\text{Th}$  series) events and could only be interpreted as sequences from the  $^{235}\text{U}$  series if both amplitude fluctuations were unusually large and in the same direction. We conclude that at most two events might have been from the  $^{235}\text{U}$  series, all the rest being from the  $^{232}\text{Th}$  series.

The amplitude and timing distributions of these events were examined in detail. Fig. 5(a) shows the amplitude distribution for the third pulse, from  $^{216}\text{Po}$ . Distributions for the other pulses were similarly narrow, showing that most decays occur within the crystal volume. The few low-amplitude events are quite close to the peak so there is no clear evidence of any contribution from surface contamination. The presence of significant numbers of events with amplitudes well above the peak is unexpected; the first and second pulses also showed this effect. It was found that the amplitudes of each of the three pulses varied by more than  $\pm 10\%$  about its mean value although the ratios of the three varied by less than  $\pm 4\%$ . In Fig. 6 we plot the summed amplitudes of the second and third pulses against their difference. The strong correlation between successive pulses is not surprising as all three alpha decays occurred at the same crystal site. However the large variation in

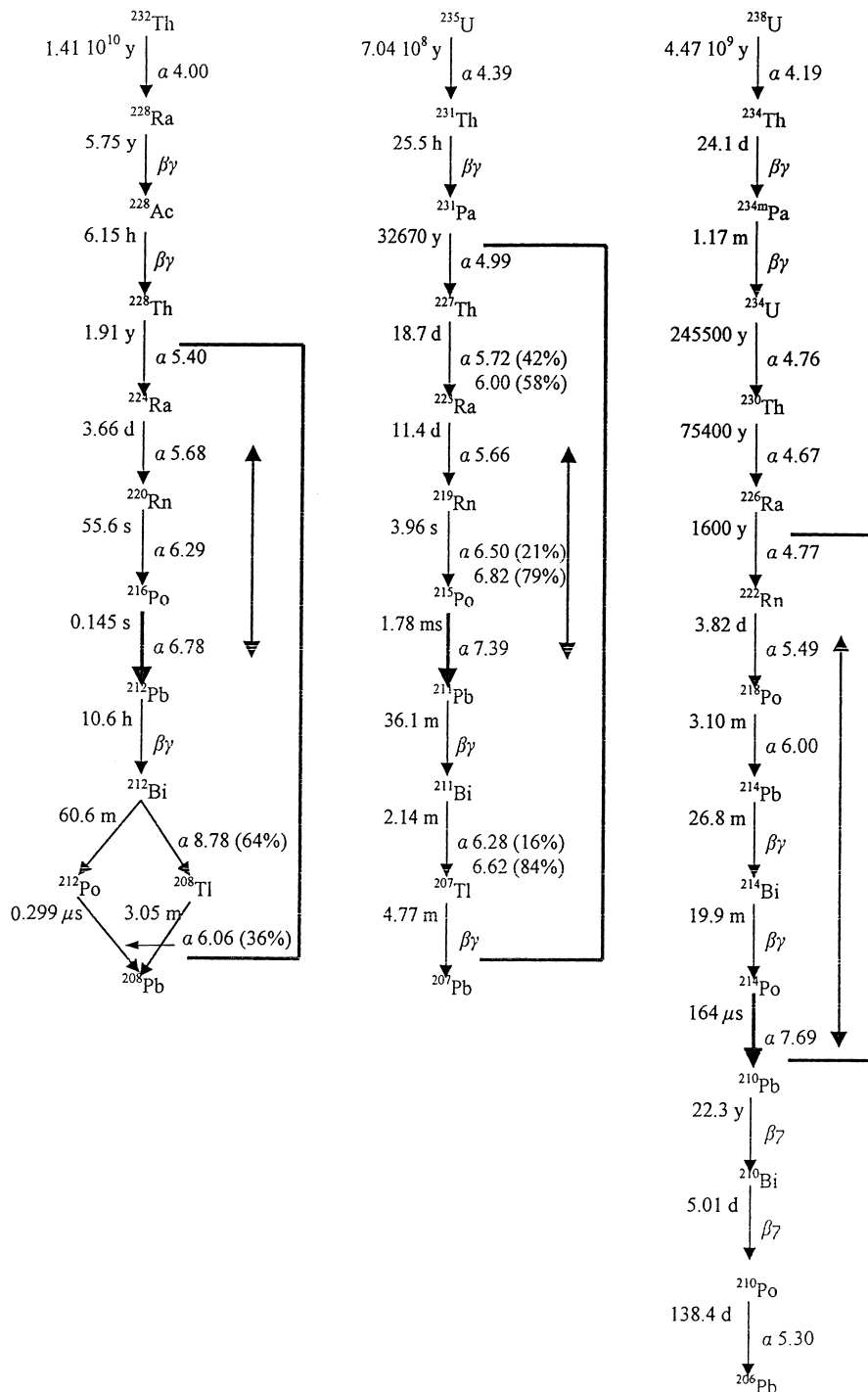


Fig. 4. Decay series of  $^{232}\text{Th}$ ,  $^{235}\text{U}$  and  $^{238}\text{U}$ ; rare ( $< 1\%$ ) branches are ignored, and average energies given for alpha decays with fine structure. Bold arrows indicate decays of short-lived alpha-emitters included in the selected  $\alpha$ - $\alpha$  or  $\beta$ - $\alpha$  coincidences, double-headed arrows the sequences of prior decays that can be observed and counted. The rectangular bars enclose those nuclei which have half-lives short compared with the duration of the experiment.

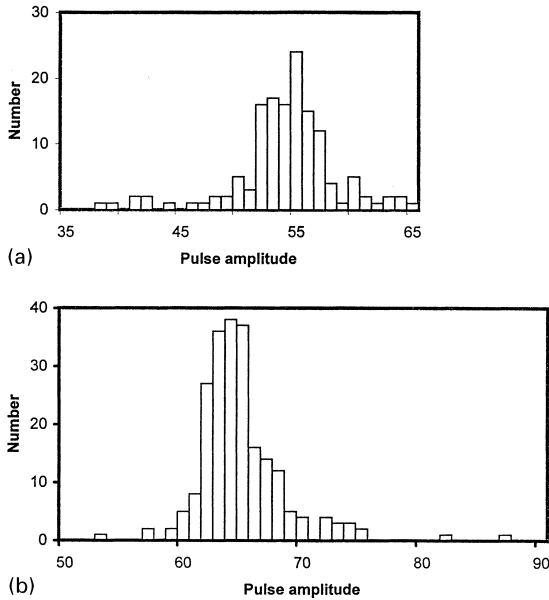


Fig. 5. Pulse amplitude distributions for alpha decays of (a)  $^{216}\text{Po}$  and (b)  $^{214}\text{Po}$ .

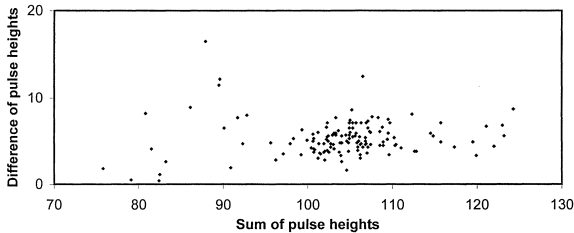


Fig. 6. Amplitude correlation of pulses from successive alpha decays in the  $^{232}\text{Th}$  series.

amplitude from event to event indicates that the overall efficiency at different locations in the crystal was not constant. This is surprising as the presence of the light guide should have smoothed out variations in the optical collection efficiency. A similar effect has been found in other crystals examined, suggesting that quite large variations in scintillation efficiency between microscopic ( $\mu\text{m}$ -sized) regions are not uncommon, some regions having efficiencies up to 20% above the average.

The timing distributions gave estimates for the relevant half-lives of  $55.8 \pm 5.6$  s ( $^{220}\text{Rn}$ ) and

$138 \pm 14$  ms ( $^{216}\text{Po}$ ), compatible with the expected values.

### 3.2. $\beta$ - $\alpha$ pairs: the $^{238}\text{U}$ series

There were 223 of these of which accidentals would account for about 5. Taking the dead time of  $75 \mu\text{s}$  into account, the relative time distribution was compatible with the  $^{214}\text{Po}$  half-life of  $164 \mu\text{s}$ . The amplitude distribution for the alpha pulses (Fig. 5b) showed similar features to those of the  $^{232}\text{Th}$  alpha sequences, with a similar high-amplitude tail. Identification of the two preceding alpha decays,  $^{222}\text{Rn}$  and  $^{218}\text{Po}$ , is complicated as there are two  $\beta$ -decays between them and the  $\beta$ - $\alpha$  trigger. A period of 3000 s was examined but in only about a third of the events could the two alpha pulses be identified unambiguously. These events were sufficient to check the half-life of  $^{218}\text{Po}$ , which was found to be  $239 \pm 36$  s, and to deduce the pulse height distributions of both decays.

### 3.3. Energy calibration of alpha pulses

The analysis described provided mean pulse amplitudes (omitting the extreme tails of the distributions in each case) for six different alpha energies  $E$ . The values are plotted in Fig. 7. The variation is close to linear but is better fitted by a quadratic form which also passes through the origin and is used in all subsequent analysis:

$$\text{pulse amplitude} = 5.80E + 0.342E^2.$$

## 4. Interpretation of the alpha particle energy spectrum

The aim is to determine the proportions of events due to each series and the extent to which the series have reached radioactive equilibrium. Consider first the  $^{232}\text{Th}$  series. The square brackets in Fig. 4 embrace all nuclei whose half-lives are short compared to the duration of the experiment. We therefore know that if any one of the five alphas is recorded then the other four must also have been present. Using the measured amplitude distributions for each decay of the  $^{224}\text{Ra}$ - $^{220}\text{Rn}$ - $^{216}\text{Po}$

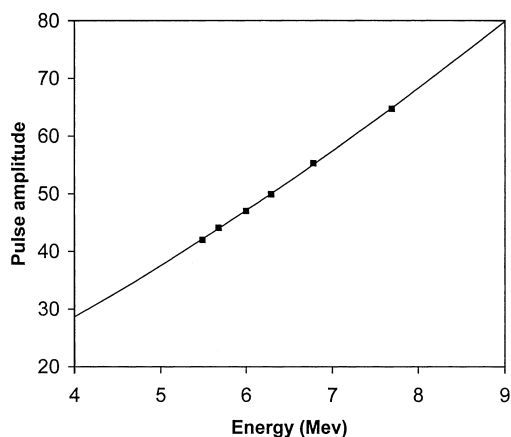


Fig. 7. Calibration curve for alpha pulses in this scintillator.

sequence, and the energy calibration curve, the distributions for the  $^{212}\text{Bi}$  and  $^{212}\text{Po}$   $\alpha$ -decays can be estimated and the expected summed distribution for the whole series (excepting the long-lived parent  $^{232}\text{Th}$ ) can be reconstructed. The short half-life of  $^{212}\text{Po}$  implies that some of the energy of the preceding  $\beta$ -decay will be added to the alpha pulse. The effect is small and as this part of the spectrum is not critical to the subsequent argument, no correction has been attempted. A correction of 2% has been applied to allow for pairs lost in the data transfer dead time.

Data for the  $^{238}\text{U}$  series are treated similarly but there are additional complications. Only four of the eight alpha particles are necessarily associated while that from  $^{210}\text{Po}$  may or may not be present depending on the age of the scintillator. The crystal used here was purchased about 15 years ago but it may have been grown considerably earlier. We therefore calculated a separate amplitude distribution for the  $\alpha$ -decay of  $^{210}\text{Po}$ . Also, the efficiency for detecting the  $\beta$ - $\alpha$  pairs is reduced, first by the trigger dead-time of 75  $\mu\text{s}$  which causes 0.27 of the events to be lost, and secondly by the failure to record  $\beta$ -decays depositing small amounts of energy. Using the  $^{214}\text{Bi}$  spectrum published by Iwawaki et al. [11] we estimate the loss due to this effect to be  $0.25 \pm 0.05$  for our threshold of 0.75 MeV. Taking these effects into account we reconstruct the expected summed distribution for

the series, excepting the long-lived parents  $^{230}\text{Th}$  and  $^{234,238}\text{U}$ .

The expected summed distributions for the relatively short-lived members of both series are added and compared in Fig. 8 with the observed alpha particle spectrum. The contribution from  $^{210}\text{Po}$  is shown on the assumption that it was present at 50% of its equilibrium value, this choice being based on the approximate age of the scintillator.

It is immediately evident, from the absence of a large excess of events in channels 30–40 corresponding to alpha energies  $< 5$  MeV from  $^{230}\text{Th}$  and  $^{234,238}\text{U}$ , that the other alpha emitters in the series cannot be present in anything approaching their equilibrium values. It is also clear, from the modest but persistent continuum contributions up to and beyond the largest alpha energies, that other processes are contributing. At the highest energies these must be due to cosmic ray events, either from the tail of the nucleonic cascade or from neutrons produced by muons. It is known [12] that the spectrum of neutrons at sea level varies as  $E^{-2}$  so we expect their contribution to increase at lower energies. Possibly, alpha particles from encapsulating material also contribute to the low-energy spectrum, though comparison of the present results with those obtained using the same scintillator at a deeper site suggests that most of the background is due to cosmic rays.

## 5. Discussion

We have shown that it is possible, by multi-parameter analysis using fast digital techniques, to determine the separate contributions of short-lived alpha emitters to the background count rate in a scintillator. The technique allows tests of the assumption of secular equilibrium in natural radioactive series. In particular, most of the alpha particle activity in the large crystal studied here is due to  $^{226}\text{Ra}$  and its relatively short-lived daughters in the uranium series, and to  $^{228}\text{Th}$  and its daughters in the thorium series, with very little contribution from the long-lived parents  $^{234,238}\text{U}$  and  $^{230}\text{Th}$ .

By measuring events which they attributed to spontaneous fission of  $^{238}\text{U}$ , Omori, Braoudakis and Peak [13] came to the opposite conclusion,



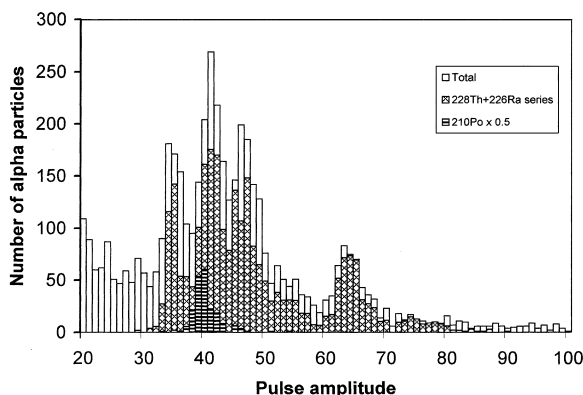


Fig. 8. The observed total alpha particle spectrum and the contributions from the two main radioactive series, excluding their long-lived parents.

namely that in their NaI scintillators  $^{238}\text{U}$  was present in much greater quantity than estimated from alpha counting and the assumption of secular equilibrium. As one possible explanation, they pointed to the unreliability of alpha counting; the technique we describe overcomes such difficulties and puts alpha assay on a firm quantitative basis.

The process of growing scintillating crystals from molten alkali halide should not greatly alter the relative partition of radium, thorium and uranium. Reasons for secular disequilibrium may therefore lie in the geochemistry of the feedstock minerals. The presence or absence of particular isotopes from the natural radioactive series may depend on the solubility of their elemental compounds. Ivanovich and Harmon [14] have stressed the relevance of the great solubility of compounds of radium to its presence in mineral deposits. Thorium, on the other hand, is one of the elements least likely to stay in solution so it is probable that the thorium series alpha emitters measured in this work derive from  $^{228}\text{Ra}$ . Since its half-life is only 5.75 years the background would have been much higher when the crystal was first purchased. (Kilgus and Kotthaus [15] reached a similar conclusion for thorium in a CsI(Tl) crystal, by measurements extending over many years.) The current thorium series activity in this crystal is deduced from the number of  $\alpha$ - $\alpha$  pairs to be  $1.4 \times 10^{-5} \text{ Bq kg}^{-1}$  with an uncertainty of about 10%.

For the uranium series the corresponding figure is  $4.5 \times 10^{-5} \text{ Bq kg}^{-1}$ , corresponding to a mass concentration of  $^{226}\text{Ra}$  of  $(2.8 \pm 0.3) \times 10^{-18}$ . The absence of evidence for alpha decays of 4.19 MeV allows an upper limit for the activity due to long-lived alpha emitters to be set at one tenth of this value, that is  $< 5 \times 10^{-6} \text{ Bq kg}^{-1}$ , equivalent to a  $^{238}\text{U}$  concentration of  $1 \times 10^{-12}$ . Although lower concentrations of uranium have been reported in the literature, they have been based either on mass spectroscopy or on the assumption, shown here to be incorrect, that the series has been in secular equilibrium. We have also noted that products of  $^{235}\text{U}$  could not be identified positively in this scintillator.

Two other NaI(Tl) scintillators we have examined, from different manufacturers, contain  $^{210}\text{Pb}$ , revealed by the 5.3 MeV alpha decay of  $^{210}\text{Po}$ . The lead is present in very small amounts (less than  $10^{-18}$  parts by weight) but it would have been detected in the scintillator studied here had it been present, even at much lower levels.  $^{210}\text{Pb}$  is known to occur in rainwater and its presence in these other crystals may be related to chemical processing of the feedstock.

Clearly the detailed analysis of the isotopes present in a scintillator is a somewhat complex procedure. Nevertheless the present method should be useful for large crystals grown from more carefully refined materials, as impurity levels at least one order of magnitude less could be measured.

## References

- [1] H. Ejiri et al., Nucl. Phys. A 611 (1996) 85.
- [2] R. Bernabei et al., Phys. Lett. B 389 (1996) 757.
- [3] K. Fushimi et al. Nucl. Phys B (Proc. Suppl. 48) (1996) 70.
- [4] P.F. Smith et al., Phys. Lett. B 379 (1996) 299.
- [5] J.C. Barton, I.M. Blair, J.A. Edgington, in: N.J.C. Spooner (Ed.), Proceedings of International Workshop on the Identification of Dark Matter, Sheffield, UK, 1996, World Scientific, Singapore, 1997, pp. 391–396.
- [6] J.C. Barton, Appl. Radiat. Isot. 47 (1996) 997.
- [7] E. Gatti, Rendiconti del seminario Mat., Fisico di Milano 31 (1961) 29.
- [8] F. Martini, E. Gatti, Energia Nucleare 9 (1962) 160.
- [9] J. Basilio Simões, C.F.M. Loureiro, J. Landeck, C.M.B.A. Correia, IEEE Trans. Nucl. Sci. NS-44 (3) (1997) 407.

- [10] R.B. Firestone, in: V.S. Shirley (Ed.), *Table of Isotopes*, 8th Edition, Wiley, New York, 1996.
- [11] T. Iwawaki, K. Fushimi, T. Horikawa, N. Koori, S. Nayakama, in: S. Sasaki et al. (Eds.), *Proceedings of 11th Workshop on Radiation Detectors and Their Uses*, Tsukuba, Japan, 1997, (KEK Proceedings 97-8) pp. 66–73.
- [12] A.O. Sanni, *Nucl. Instr. and Meth.* 137 (1976) 517.
- [13] M. Omori, G. Braoudakis, L.S. Peak, *Nucl. Instr. and Meth. A* 329 (1993) 183.
- [14] M. Ivanovich, R.S. Harmon, *Uranium Series Disequilibrium: Application to Environmental Problems*, 2nd Edition, OUP, Oxford, 1992.
- [15] U. Kilgus, R. Kotthaus, *Nucl. Instr. and Meth. A* 365 (1995) 581.